JOURNAL OF MATERIALS SCIENCE 23 (1988) 782–789

Microstructural transformations in austenitic–ferritic transition joints

F. GAUZZI, S. MISSORI
Department of Mechanical Engineering, University of Rome 'Tor Vergata', via Orazio Raimondo, 00173 – Rome, Italy

The relatively complex microstructures developed at the interface between ferritic steel and weld metal on austenitic–ferritic transition joints have been examined by metallographic observation and by hardness tests in the as-welded condition and in the as-welded-and-tempered condition. Both austenitic stainless steel and nickel-based filler metals were used in welds. On as-welded specimens a sharp change of hardness in low-alloy steel has been measured, with increasing distance from weld metal; the hardness values have been related to the observed metallographic constituents. On post-weld heat treated specimens, the behaviour is different according to the composition of filler material, either austenitic steel or nickel-based alloy. In the case of austenitic filler material, a dark-etching narrow diffusion region of carbon toward weld metal is formed, with an adjacent markedly decarburized zone, exhibiting the minimum microhardness values in a narrow band of about 60 micrometres. Since this sharp structural variation is recorded just in the zone where often failures occur, the final post-weld heat treatment appears to be proposed with due caution. In the case of nickel-based filler material, carbon diffusion is inhibited by the precipitation of alloy carbides at the weld interface. This determines a more homogeneous heat affected zone (HAZ) in the ferritic steel and a reduced decarburization near the fusion line after a post-weld heat treatment, confirming the reasons of the preference recognized to this filler material, especially when service temperature is elevated and submitted to frequent changes, or whenever a post-welded heat treatment is required.

1. Introduction

Transition joints between austenitic stainless steels and ferritic steels are commonly employed in fossil-fired power plants. For economy purposes, low-alloy ferritic steels (especially 2.25Cr–1Mo steels) are used wherever possible to make parts such as primary boiler tubing, operating at moderate temperatures. Instead, the more oxidation-resistant austenitic stainless steel are used for parts submitted to higher temperatures, such as final stages of boiler superheater and reheater sections. Thus transition joints are required.

Most transition joints are carried-out on small-diameter tubing. A steam boiler in a power plant can contain some thousands of joints, operating at temperatures between 500 and 550° C, with a service pressure of about 16 to 20 MPa. It has been estimated that at present several hundreds of thousands of transition joints are in service. Often failures occur after 15 to 20 years of operation, well before the expected life time of generator is achieved, thus causing economic losses consequent upon power plant shutdown and necessity of repairing damaged tubing [1].

The interest in transition joints is nowadays increasing owing to their inclusion in nuclear power plants [2, 3].

Prolonged exposure of transition joints to elevated temperatures poses a lot of metallurgical and mechanical problems, recognized for years, which can be summarized as follows:

1. difference between expansion coefficients of austenitic and ferritic steels can develop, because of start-up and shut-down of plant, high cyclic stresses at the interface of dissimilar metals, with possible low-cycle fatigue;
2. the heat affected zone (HAZ) of the ferritic steel component is substantially weakened by the carbon migration from the HAZ toward the weld metal, so that large creep strength mismatch between ferritic steel and weld metal can favour creep rupture;
3. the low oxidation-resistance of ferritic steel at elevated temperature may increase susceptibility to low ductility failure for oxide notch-effect.

Austenitic stainless steels and nickel-based filler metals are commonly utilized for fusion welds. For austenitic materials the coefficient of thermal expansion is about 40% higher than that of ferritic steels, thus inducing elevated thermal stresses at the ferritic steel-weld metal interface. For nickel-based weld materials the expansion coefficient is intermediate between those of the two materials to be joined, and closer to that of ferritic steel. Therefore the

0022–2461/88 $03.00 + .12

TABLE I Characteristics of materials used

	Chemical composition (%)								Tensile strength* (MPa)
	C	Mn	Si	Cr	Mo	Ni	P	S	
2.25Cr–1Mo steel (normalized and tempered)	0.10	0.60	0.27	2.28	0.93	–	0.011	0.013	681
AISI 304L steel (solution treated)	0.02	1.56	0.56	18.1	–	10.0	0.028	0.001	594

*Measured at room temperature.

preference recognized to the latter filler material is justified.

Several authors have highlighted the major role of fluctuating stresses in the failure mechanism. The high thermal stresses at the interface consequent upon repeated start-up and shut-down could give rise to a low-cycle fatigue failure [1, 4].

Some other authors have pointed out the occurrence of creep damage in the ferritic steel, considering the different behaviour and strength of the weld metal and ferritic steel. Experimental work has demonstrated the possibility of obtaining low-ductility creep failures through accelerated rupture tests [5, 6].

It has been widely recognized the substantial contribution of metallurgical deterioration due to exposure at elevated temperature. Failures have occurred in most of cases in the HAZ of the ferritic steel, at a distance of few micrometres or few tens of micrometres from the fusion boundary.

To improve the thermal behaviour of transition joints, several methods have been proposed, such as:

1. using transition or spool pieces made of a material with a coefficient of expansion intermediate between austenitic and ferritic steels [7]. It may be argued however that this method is too expensive and can even result in a greater risk of failure, due to the larger quantity of welds involved and relevant possible defects. Alloys 46Fe–32.5 Ni–21 Cr (UNS N08800) and 43Fe–36 Ni–19Cr (UNS N08330) have been proposed;
2. using an oxidation-resistant coating applied on the external surfaces of welds; in this case the difficulty of keeping a sound and crack-free coating has to be overcome, in spite of thermal stresses arising from expansion differences between coating and coated metals;
3. avoidance or reduction of secondary stresses (due to bending, vibrations, etc.) along sections of tubing containing transitions joint.

Research proceeds with the aim of investigating failure mechanisms, studying microstructural evolutions of materials after exposure at elevated temperature, determining experimental criteria to estimate the lifetime of joints, improving mechanical properties through better welding techniques and new filler materials [1, 4, 6–9].

The present paper has the purpose of giving a contribution to the study of metallographic structures of fusion joints, carried out with different filler materials, including effects of post-weld heat-treatment.

2. Experimental procedure

Two butt welds were carried out using 10 mm thick 2.25Cr–1Mo and AISI 304L steel plates. The filler materials were either AISI 309 (austenitic stainless steel) or INCO-WELD A (nickel-based alloy). The chemical composition and tensile strengths of base and filler materials are shown in Tables I and II. Welding parameters are given in Table III.

Before starting welding operations, a preheat to about 150° C was performed, and a minimum temperature was kept between each pass and the next one.

After completion, weldments were submitted to non-destructive tests (dye penetrant and radiographic inspections) without revealing welding defects. One part of the weldment was submitted to a post-weld treatment of stress-relief and tempering at 730° C for 2 h, the other one was left in the as-welded condition (Table IV).

Several specimens for mechanical tests and metallographic examination were machined from each weldment.

Results of the tensile tests on transversal specimens cut from each weldment are listed in Table V. The section of specimens was 9 mm × 10 mm, with a useful length of 70 mm. The values of the tensile strengths were intermediate or lesser in comparison with those of ferritic steel and austenitic stainless steel. Specimens 1, 2 and 3 showed a slight strengthening on the AISI 304L side, equal to about 7%, which was attributed to a favourable effect of welding residual stresses,

TABLE II Characteristics of filler metals

	Typical all-weld metal composition (%)											Tensile strength* (MPa)
	C	Mn	Cr	Si	Ni	Mo	P	S	Cu	Nb	Fe	
AISI 309 (rod)	0.10	1.5	24	0.7	13	–	0.02	0.02	0.5	–	bal.	986
INCO-WELD A (electrode)	0.10	2.0	15	0.3	70	1.5	–	0.02	0.5	1.8	9	995

*Measured at room temperature on specimens made from filler metal.

TABLE III Welding procedures

	Weldment 1	Weldment 2
Filler material	AISI 309	INCO-WELD A
Welding process	Gas tungsten arc	Manual metal arc
Diameter of electrode (mm)	–	3.2
Diameter of rod (mm)	2.0	–
Current (A)	170	110
Argon flow rate (dm sec^{-1})	0.2	–
Preheat and interpass temperature (° C)	150	150

probably arising from the severe restraint conditions of weldment. The weakening of the 2.25Cr–1Mo side on specimen 4 was attributed to an expected softening effect of post-weld heat treatment.

Results of the tensile tests on longitudinal specimens machined along ferritic steel HAZ only, in order to evaluate tensile properties of the HAZ, are shown in Table VI. The section of specimens was 5 mm × 2 mm, with a useful length of 25 mm (according to metallographic observation, a width of 2 mm has been chosen to represent the average tensile properties of the HAZ). Due to the severe hardening which occurred during welding, tensile strengths in the HAZ resulted in rather higher values.

To investigate the microstructural tranformations, macrohardness and microhardness tests on the various specimens were performed, by measuring values with increasing distances from the fusion boundary. Vickers' macrohardness test was used, with a test load of 10 Kgf and a loading time of 20 sec. The microhardness test was also Vickers, with a load test of 50 gf and a loading time of 10 sec.

3. Development of microstructures

The ferritic steel 2.25Cr–1Mo utilized for weldments was supplied after normalizing at 900° C, followed by tempering at 700° C. The former treatment gives rise to the development of bainite mixed to martensite, the latter treatment transforms such a structure to ferrite with carbides (Fig. 1).

During welding a region next to the fusion line is heated up in a short time to an elevated temperature exceeding Ac_3 (Ac_3 = line in Fe–C diagram showing thermal arrest resulting from the transformation ferrite → austenite on heating.) Microstructural changes occurring in the HAZ of ferritic steel depend on the kinetics of austenite formation, on austenite grain size and on the CCT (CCT = Continuous Cooling Transformation) diagram of the steel [10]. Since the locally attainable maximum temperature and cooling rate decrease as distance from melted material increases, it is theoretically possible to forecast the formation of three zones in a single pass weld.

TABLE IV Post-weld heat treatment (PWHT)

Type	Max temperature (° C)	Holding time at max temperature (h)
Stress relief and tempering	730*	2

*Heating and cooling in furnace.

1. a first zone where the austenite developed during heating over Ac_3 gives rise to a mixed bainite–martensite structure with a coarse grain;
2. a second zone where the peak temperature, still over Ac_3, is lower and the resulting structure, bainite with martensite, is fine-grained;
3. a third zone where the temperature is raised to a value between Ac_1 and Ac_3, with partial austenitization and development at the cooling of a mixture of transformation structures of prior austenite, starting from the grain boundaries and delimiting parts of untransformed material.

Metallographic observations on specimens machined from weldments, has shown that the ferritic steel HAZ structure, resulting from multipass welding operations, can be often more complex and commonly includes bainite + martensite, possibly tempered, and pro-eutectoid ferrite.

The effect of the multipass technique is that of submitting the structures formerly developed to one or more thermal cycles with their possible tempering. Under a given configuration (welding thermal input, preheat temperature, size of piece, etc.), by decreasing the distance from melted zone formed at each pass:

– the peak temperature reached in the HAZ increases;
– the holding time at elevated temperature increases as well.

Because of this, the degree of tempering of the

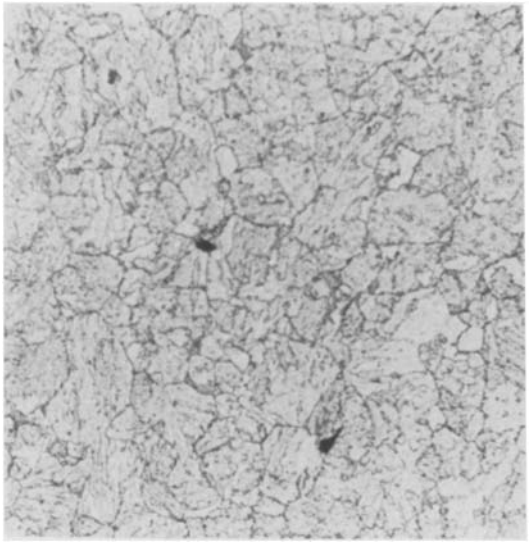

Figure 1 Microstructure of as-supplied low-alloy ferritic steel (normalized and tempered). Ferrite with little bainite (HV_{10} = 221).

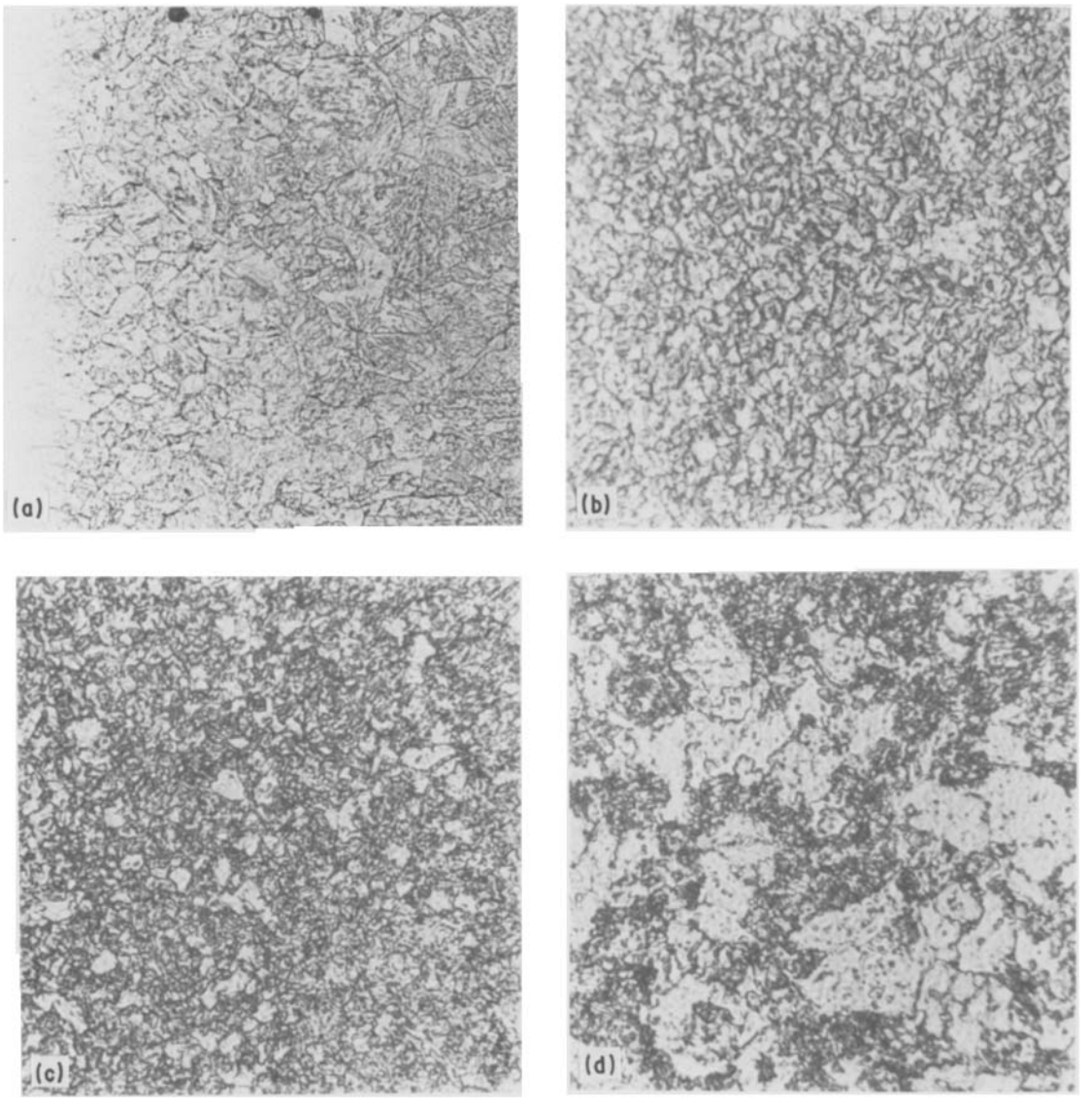

Figure 2 HAZ microstructures of low-alloy ferritic steel. Specimens cut from Weldment 1 (Table III) as-welded, etched in nital: (a) weld interface (400 ×). HV_{10} = 383 at 0.15 mm from interface. (b) distance from weld interface: 0.75 mm – Bainite + martensite (1000 ×). HV_{10} = 421. (c) distance from weld interface: 1.25 mm – Bainite + martensite, with some amount of pro-eutectoid ferrite (1000 ×). HV_{10} = 403. (d) distance from weld interface: 2.25 mm – Ferrite with coalesced carbides (1000 ×). HV_{10} = 254.

formed structures is variable according to the distance from the melted zone. Thus the structures present sharp changes with increasing distance from the fusion boundaries and an asymmetry along the thickness, depending on the welding technique and the sequence of passes.

Metallographic observation using an optical microscope allowed the identification, along the middle of plate thickness of Weldment 1, the following structures in the ferritic steel HAZ (Fig. 2):

1. an interface between weld metal and ferritic steels;
2. a first zone showing a bainitic structure, mixed to martensite, about 0.2 mm wide, with a hardness quite high in comparison with the prior hardness of steel (Fig 2a);
3. a second zone also showing a bainite–martensite structure, but fine-grained, about 1 mm wide, with the maximum values of hardness (Fig. 2b);
4. a third zone having a bainite–martensite structure

TABLE V Results of tensile tests on transversal specimens machined from weldments (tests made at room temperature)

Specimen	Filler material	Heat treatment	Tensile strength (MPa)	Failure	
				Location	Distance from weld metal
1	AISI 309	as-welded	620	on weld metal	–
2	AISI 309	PWHT	605	at interface weld metal/2.25Cr–1Mo	–
3	INCO-WELD A	as-welded	637	on AISI 304L steel	22 mm*
4	INCO-WELD A	PWHT	580	on 2.25Cr–1Mo steel	18 mm*

*Measured after elongation.

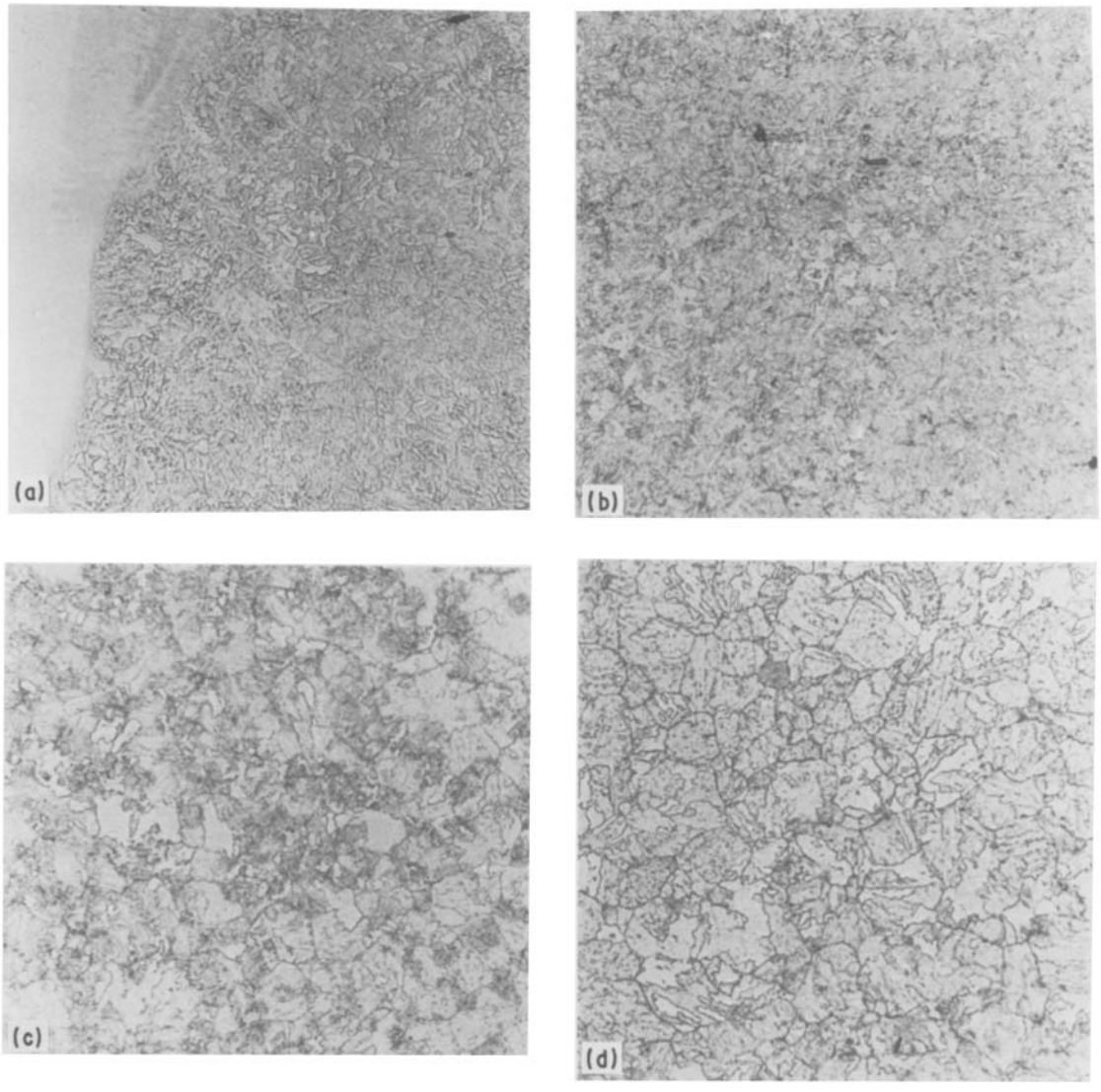

Figure 3 HAZ microstructures of low-alloy ferritic steel. Specimens cut from Weldment 2 (Table III) as-welded, etched in nital (400 ×): (a) weld interface. HV_{10} = 309 at 0.15 mm from interface. (b) distance from weld interface: 1 mm – Bainite with little martensite. HV_{10} = 336. (c) distance from weld interface: 2 mm – Bainite with ferrite. HV_{10} = 336. (d) distance from weld interface: 3 mm – Ferrite with bainite. HV_{10} = 254.

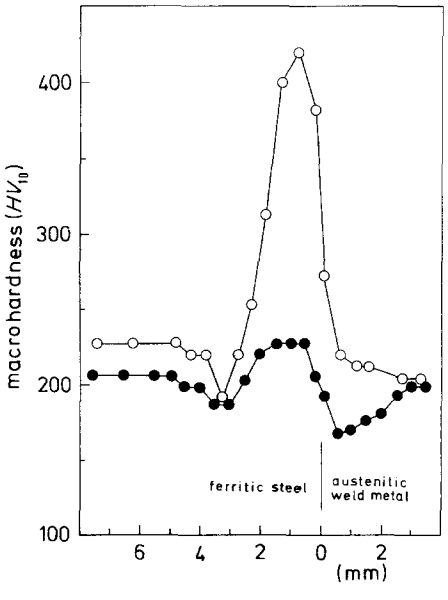

Figure 4 Macrohardness profiles for specimens welded by using austenitic stainless steel filler material. (○) as-welded, (●) stress-relieved and tempered.

mixed to pro-eutectoid ferrite (deriving from prior ferrite, not transformed during the welding thermal cycles, approximately 0.5 mm wide, with hardness values still elevated (Fig. 2c);

5. one transition zone, consisting of ferrite mixed with coalesced carbides, about 1 mm wide, with hardness values intermediate between those of base materials and the maximum values in the HAZ (Fig. 2d);

6. the last zone, showing the same features as the base material, practically unaffected, with a minimum hardness at 3 or 4 mm of distance from the fusion boundary (Fig. 1).

TABLE VI Results of tensile tests on HAZ longitudinal specimens (tests made at room temperature)

Specimen	Filler material	Heat treatment	Tensile strength (MPa)
1	AISI 309	as-welded	1092
2	INCO-WELD A	as-welded	962

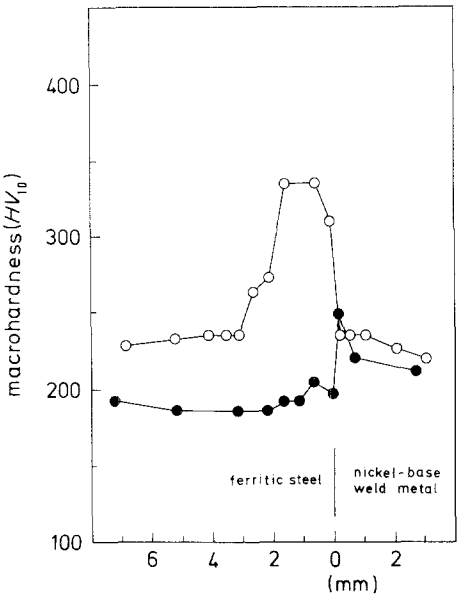

Figure 5 Macrohardness profiles for specimens welded by using nickel-based filler material. (○) as-welded, (●) stress-relieved and tempered.

On Weldment 2 the width of the ferritic steel HAZ was slightly larger and the measured values of hardness presented a lower maximum value and a less sharp trend compared with the values recorded on specimens made from Weldment 1. An explanation of this difference has been given taking into account the faster cooling of Weldment 1 due to the protection argon flow, used also on the back during the first two welding passes. Moreover, a slightly higher heat input of welding procedure for Weldment 2 could have occurred, in connection with a slower speed of the welding arc. These two circumstances should have determined a slightly greater hardening in the HAZ of Weldment 1. Some of the observed microstructures are shown in Figs 3a to d.

4. Evolution of microstructures at high temperatures

To evaluate the effects of the temperature on microstructures, specimens submitted to a post-weld heat treatment for stress-relieving and tempering (see Table IV) have been examined. The hardness values (HV_{10}) measured after post-weld heat treatment are shown in Figs 4 and 5 for joints carried out with austenitic stainless steel and nickel-based alloy, respectively; for comparison, hardness values on as-welded specimens are reported. According to the composition of the filler material, the weld metal is either of austenitic steel or nickel-based type. After exposure at high temperature and because of the mismatch of chemical composition across the interface, transformations occur, due to solid state diffusion.

The different activity of carbon in the ferritic steel and the weld metal gives rise to a migration of carbon toward the fusion line, with formation of precipitates in the weld metal and carbon depletion of the ferritic steel HAZ. It is also presumed that alloy elements contained in the weld metal (Cr, Ni, Mo, etc.) diffuse toward the ferritic steel, with a resulting increase of their content in the ferritic steel HAZ. In this case diffusion could partially balance the weakening caused by carbon migration.

With specimens welded using austenitic steel filler metal, submitted to post-weld heat treatment for stress-relieving and tempering at 730° C for 2 h, it is possible to observe (Fig. 6) the formation of a narrow region, appearing dark after etching, extending from the interface toward the weld metal with a mean width of $\sim 50\,\mu$m. The line of separation, coinciding with interface, appears clearly outlined; instead it is very indistinct on the side of austenitic weld metal. A decarburized area is evident in the ferritic steel, nearly completely free from precipitated carbides, having a width approximately equal to the adjacent narrow dark-etching region. In order to show the hardness decrease at the interface dark-etching zone/decarburized zone, microhardness tests were made. Fig. 7 shows a row of microhardness test points; the correspondent profile is reported in Fig. 8. Moving toward the weld metal, are visible precipitates at the boundaries of stainless steel austenitic grains. From the observation of metallographic appearance (See Figs 5,

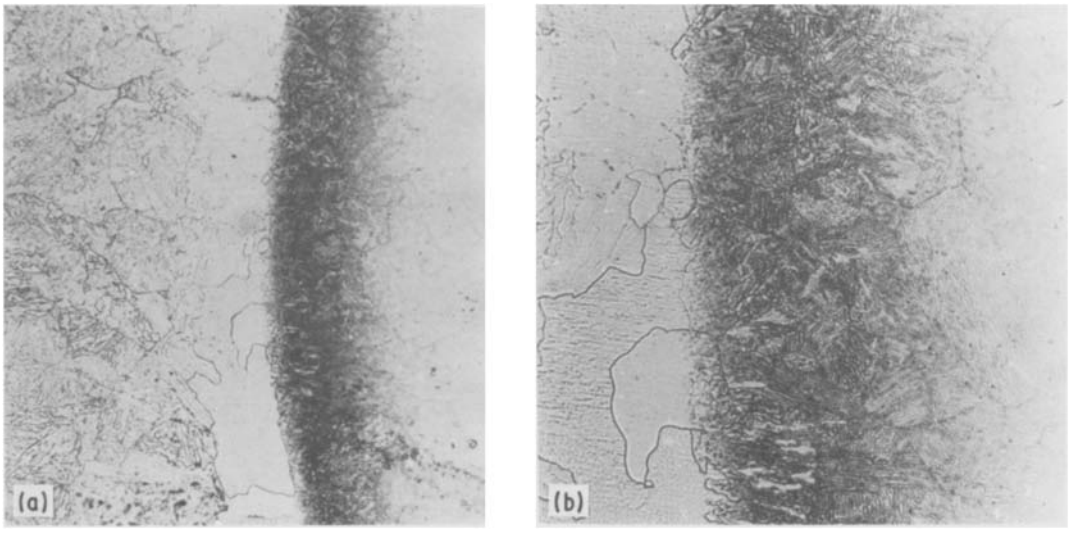

Figure 6 Post-weld heat treated specimens, welded by austenitic stainless steel filler material, etched in nital: (a) Weld interface (200 ×). Metallographic appearance of the dark etching area with the adjacent decarburized narrow band. (b) Detail of the dark area in (a) (400 ×). Coarse and malformed lamellae of pearlite are shown.

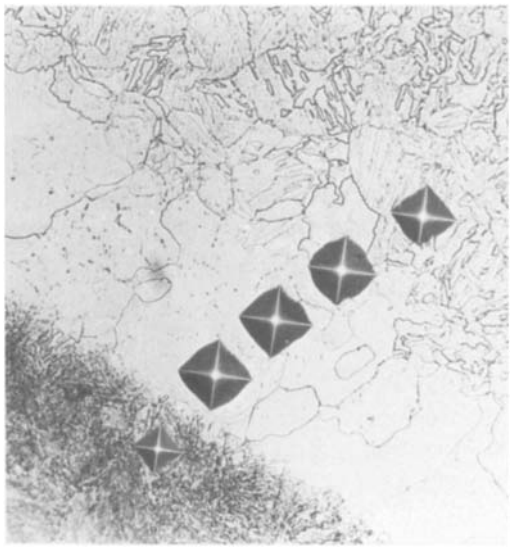

Figure 7 Microhardness tests on decarburized and dark-etching zone on specimen made from Weldment 1, etched in nital (400 ×).

Figure 9 Microstructure of post-weld heat treated low-alloy steel, far from weld interface, etched in nital. Ferrite with little bainite and dispersed carbides (500 ×). HV_{10} = 206.

6 and 7) and consideration of the elevated microhardness values ($\sim 400\ HV_{50gf}$) compared with the nearby ferritic zone ($\sim 150\ HV_{50gf}$), the dark region is believed to be a narrow diffusion area of carbon within the austenitic matrix of weld metal. The concentration of carbon and the Cr/Ni ratio in the narrow diffusion region assumes such a value as to induce a pearlitic transformation. The resulting microstructure in the carbon-rich zone is a coarse pearlite, in which the presence of malformed lamellae can be observed, characterizing chromium-rich pearlite. Such precipitates, not formed during the welding operations due to the short time interval within the critical temperature range, can develop after sufficient exposure at high temperature during the post-weld heat treatment. With increasing distance from the weld metal, the ferritic steel structure appears to mainly consist of ferrite with dispersed carbides (Fig. 9).

With specimens welded using a nickel-based filler material, the weld metal is composed of a stable austenitic-type solid solution, but very rich in nickel; so development of pearlite is inhibited. With these specimens, a narrow dark-etching region has also been observed at the interface, but its appearance is thinner and less marked; in addition, the microstructure of the heat affected zone on ferritic steel is more homogeneous due to reduced decarburization (Fig. 10). This is confirmed by the microhardness profile at the interface (Fig. 8).

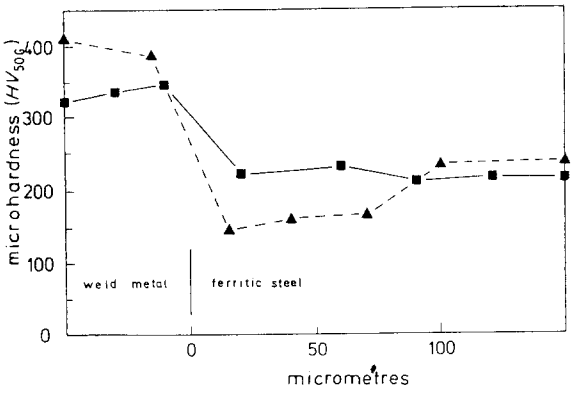

Figure 8 Microhardness profiles on post-weld heat treated specimens. (△) Stainless steel filler metal, (□) nickel-base filler metal.

5. Conclusions

(a) The examination of the heat affected zone of ferritic 2.25Cr–1Mo steel in the as-welded condition allowed observation of mixed bainite–martensite microstructures, presenting peak hardness values (about 350–400 HV_{10}) larger than in the steel in the as-supplied condition (about 200 HV_{10}, after normalizing and tempering). The hardness increase can be rather variable according to the welding procedure parameters (heat input, argon flow rate, if provided). Maximum hardness values have been recorded at some distance ($\sim 500\ \mu m$) from the fusion line. The hardness reduction at the interface with the weld metal is likely to be connected to the coarsening of the bainite–martensite microstructure, due to the elevated temperature reached near the fusion line during welding operations.

(b) Thermal ageing, which the welded joint undergoes during the post-weld heat treatment, is dependent on the composition of the filler metal.

In the case of austenitic filler material a narrow dark-etching zone, running along the bimetallic interface, and a decarburized zone in the ferritic steel have been observed. The microhardness profile on these zones showed a minimum hardness in the decarburized zone. Within the dark zone the precipitation takes place of alloy-element carbides and of pearlite, derived from the pearlitic transformation induced by the high carbon content in the ferritic steel and by the elevated Cr/Ni ratio.

In the case of the nickel-based weld metal, pearlitic transformation is inhibited; instead the formation of alloy carbides has been revealed, precipitating along fusion boundary and obstructing the carbon diffusion towards the weld metal.

The post-weld heat treatment, if provided, contributes to reduce the part of the total stress depending on the residual welding stresses. This effect would be

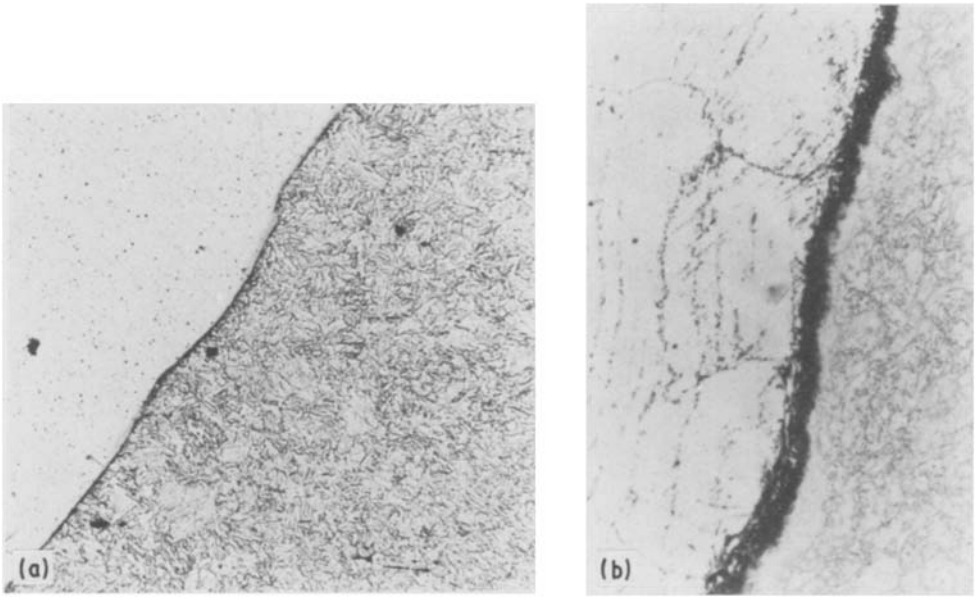

Figure 10 Weld interface on post-weld heat treated specimen welded by nickel based filler material, etched in nital: (a) Metallographic appearance of the dark etching area along interface (200 ×) (b) Detail of Fig. 10a on an overetched specimen, showing presence of precipitates also in weld metal (750 ×).

particularly beneficial for the transition zone between the two materials, in which are concentrated the stresses arising from the different expansion coefficients of the dissimilar materials occurring during the thermal cycles. Such a treatment however gives rise to a metallurgical alteration, more evident after using austenitic stainless steel filler material (carbon migration, carbide precipitation), revealed by metallographic observation and by hardness tests. In the case of the austenitic filler metal microhardness tests have shown the possible occurrence of a variation of hardness (from 150 to 400 HV_{50gf}) in a very short distance (some tens of micrometres), just in the zone where, according to several authors, failure is likely to occur during service. So a post-weld heat treatment should be proposed with due caution, especially when using austenitic filler materials.

(c) The use of nickel-based filler metals reduces decarburization near the fusion line and attenuates the microstructural variations following a post-weld heat treatment at high temperature. The advantageous behaviour, in addition to the above mentioned reduction of thermal stresses, further justifies the preference recognized to nickel-based filler materials, especially at elevated service temperatures and in the occurrence of frequent temperature changes.

References

1. R. L. KLUEH and J. F. KING, *Weld. J.* **61** (9) (1982) 302-s.
2. K. F. HALE, "Physical metallurgy of reactor fuel elements" (The Metals Society, London, 1975) pp. 193-201.
3. A. K. HARDY, T. ROWLEY and J. A. WILLIAMS, "Ferritic steels for fast breeder reactor steam generators" (British Nuclear Energy Society, London, 1978) p. 36.
4. R. L. KLUEH, J. F. KING and J. L. GRIFFITH, *Weld. J.* **62** (6) (1983) 154-s.
5. I. J. CHILTON, A. T. PRICE and B. WILSHIRE, *Met. Technol.* **11** (9) (1984) 383.
6. M. D. C. MOLES, M. J. TINKLER and H. J. WESTWOOD, *ibid.* **8** (4) (1981) 121.
7. J. F. KING, M. D. SULLIVAN and G. M. SLAUGHTER, *Weld. J.* **56** (11) (1977) 345-s.
8. R. D. NICHOLSON, *Met. Technol.* **9** (8) (1982) 305.
9. R. W. E. EMERSON, R. W. JACKSON and C. A. DAUBER, *Weld. J.* **41** (9) (1962) 385-s.
10. A. SCHRADER, A. ROSE, "De Ferri Metallographia" (Verlag Stahleisen GMBH Dusseldorf, 1966) p. 127.

Received 12 August 1986
and accepted 11 February 1987